Performance Evaluation of Space Modulation Techniques in VLC Systems

Performance Evaluation of Space Modulation Techniques in VLC Systems

Athanasios Stavridis and Harald Haas
Li-Fi Research and Development Centre,
Institute for Digital Communications (IDCOM),
School of Engineering,
The University of Edinburgh,
Edinburgh, UK
E–Mail: {a.stavridis, h.haas}@ed.ac.uk

***Abstract*—In this paper, the Bit Error Rate (BER) performance of three major space modulation techniques in a Multiple-Input Multiple-Output (MIMO) Visible Light Communication (VLC) system is studied. The considered space modulation techniques are Optical Spatial Modulation (OSM); Optical Generalized Spatial Modulation (OGeSM); and Optical Multi-Stream Spatial Modulation (OMS-SM). The space modulation techniques are evaluated against two benchmark systems: Optical Spatial MultipleXing (OSMX) and Optical Repetition Coding (ORC). The performance assessment, for both the space modulation schemes and the benchmark systems, is undertaken using simulation and analytical results. For the considered system setup, it is concluded that, in relative low Signal-to-Noise Ratio (SNR), OSM offers the best performance. Whereas, in relative high SNR and for high spectral efficiency, OMS-SM is the most efficient scheme in terms of BER.**

I. Introduction

Visible Light Communication (VLC) is a new means of wireless communication that has the potential to provide ultra high data rates [1, 2]. Recent results demonstrate that a single Light Emitting Diode (LED) is able to provide a data rate of 3 Gb/s [3]. In addition, the incorporation of Multiple-Input Multiple-Output (MIMO) techniques in a VLC system is shown to provide further improvements in the data rate [4].

The deployment of MIMO techniques in VLC is mainly inspired by the high data rate potential of MIMO systems in Radio Frequency (RF) communication [5]. However, the techniques of RF MIMO communication are not directly transferable to VLC. In fact, the nature of the optical channel presents different challenges [6]. Hence, the research of the performance of MIMO communication in VLC is important.

In this research area, several authors have studied the deployment of MIMO techniques in VLC. In [4], the concept of Spatial MultipleXing (SMX) in VLC is presented. Furthermore, in [7], the Bit Error Rate (BER) performance of several MIMO schemes in VLC is studied. Specifically, in [7], the performance of Optical Spatial Modulation (OSM) is compared against the corresponding performance of Optical Spatial Multiplexing (OSMX) and Optical Repetition Coding (ORC). In addition, the performance of OSM is also researched in [8, 9]. The incorporation of MIMO techniques that utilize Channel State Information at the Transmitter (CSIT) in VLC is presented in [10–12].

Spatial Modulation (SM) is a successful MIMO scheme in RF communication which also has been extensively studied in VLC [7, 10–13]. Due to its operating principle, SM promotes a lower complexity transceiver implementation compared to traditional MIMO schemes, such as SMX [13, 14]. Especially, at the transmitter side only one RF chain is required. This is shown to provide energy efficiency advantages [14]. Inspired by the concept of SM, several extensions of SM have been developed. For a complete introduction of the concept of SM and its variants, the reader is referred to [13].

The objective of this paper is to extend the main space modulation schemes from RF communication to VLC. Specifically, the performance evaluation of SM [13], Generalized Spatial Modulation (GeSM) [15], and Multi-Stream-Spatial Modulation (MS-SM) [16] is studied using the metric of BER. In this paper, these schemes are termed as OSM, Optical Generalized Spatial Modulation (OGeSM), and Optical Multi-Stream-Spatial Modulation (OMS-SM), respectively. Their performance is compared against the corresponding performance of two benchmark systems: ORC and OSMX. In addition, a general theoretical framework that assesses analytically the Average Bit Error Probability (ABEP) of both the studied space modulated techniques and benchmark systems is proposed. This framework is based on the union bound technique [17]. Finally, for the considered system setup, it is concluded that OSM offers the best BER performance in relative low Signal-to-Noise Ratio (SNR). However, as the spectral efficiency and SNR are increased, OMS-SM is shown to be the most efficient scheme in terms of BER.

The remainder of this paper is organized as follows: The system model of the considered VLC system is given in Section II. In addition, Sections II-A1 to II-A3 introduce the major space modulation techniques studied in this paper. The theoretical framework that assesses the ABEP of the considered space modulation schemes and benchmark systems is presented in Section III. The analytical and simulation results that evaluate the BER performance of the different VLC transmission schemes are discussed in Section IV. Finally, the concluding remarks are given in Section V.

Notation: In the following, lowercase bold letters denote vectors and uppercase bold letters denote matrices. Notation $(\cdot)^T$ denotes the transpose of a matrix. The Euclidean norm is

denoted as $\|\cdot\|_2$. The representation of the natural logarithm is given as $\ln(\cdot)$. A Gaussian distribution with mean m and variance σ^2 is represented as $\mathcal{N}(m, \sigma^2)$.

II. System Model

In this section, a VLC system which incorporates N_t LEDs and N_r Photo Detectors (PDs) is considered. Due to the nature of the Optical Wireless Channel (OWC), Intensity Modulation (IM) and Direct Detection (DD) are deployed. Usually, in VLC systems, only the Line-of-Sight (LOS) (dominant) component of the channel gain is considered [6, 7]. Therefore, the optical MIMO system equation is given as:

$$\mathbf{y} = r\mathbf{H}\mathbf{x} + \mathbf{w}, \tag{1}$$

where, $\mathbf{y}$ is the $N_r \times 1$ received signal vector. The responsivity of the PDs, in A/W, is denoted as r. Furthermore, $\mathbf{H}$ is a $N_r \times N_t$ matrix which denotes the optical channel. In more detail, the (i, j) element of $\mathbf{H}$, $i = 1, \ldots, N_r$ and $j = 1, \ldots, N_t$, which is denoted as $h_{i,j}$, represents the optical channel impulse response between the i-th receive PD and the j-th transmit LED. In addition, $\mathbf{x}$ is the $N_t \times 1$ transmitted signal vector. Each element of $\mathbf{x}$ is a positive number and represents the optical intensity transmitted from the corresponding LED. In order: i) to provide a fair comparison between the different transmission techniques; and ii) to ensure the efficient operation of the LEDs under the applied lighting constraints, the normalization of $\mathrm{E}_{\mathbf{x}}[\mathbf{x}] = P_{\mathrm{o}}$ is imposed. Here, P_{o} is the average optical transmission power. The way that the elements of $\mathbf{x}$ are selected depends on the deployed MIMO transmission technique. More detail is given in Section II-A, where all of the studied space modulation transmission techniques in this paper are presented. The composite effect of the ambient light shot and thermal noise is represented by $\mathbf{w}$. Following the assumptions of [6], $\mathbf{w}$ is modeled as real Additive White Gaussian Noise (AWGN), where $\mathbf{w} \sim \mathcal{N}(\mathbf{0}, \sigma^2_{\mathbf{w}}\mathbf{I})$. Here, it holds that $\sigma^2_{\mathbf{w}} = \sigma^2_{\mathrm{shot}} + \sigma^2_{\mathrm{thermal}}$, where σ^2_{shot} and $\sigma^2_{\mathrm{thermal}}$ denote the variance of the shot and thermal noise, respectively.

As noted, this paper focuses on a LOS VLC scenario, where only the dominant component of the channel gain is considered. Therefore, according to [6], the channel impulse response between the i-th PD and the j-th LED, $h_{i,j}$, is written as:

$$h_{i,j} = \begin{cases} \frac{A(k+1)}{2\pi d^2_{i,j}} \cos^k(\phi_{i,j}) \cos(\psi_{i,j}), & 0 \le \psi_{i,j} \le \Psi_{\frac{1}{2}}, \\ 0, & \psi_{i,j} > \Psi_{\frac{1}{2}}. \end{cases} \tag{2}$$

In (2), A is the area of each PD. Furthermore, the Lambertian factor k, which determines the directionality order, is given as:

$$k = \frac{-\ln(2)}{\ln\left(\cos\left(\Phi_{\frac{1}{2}}\right)\right)}, \tag{3}$$

where, $\Phi_{\frac{1}{2}}$ denotes the transmitter semi-angle. The distance between the i-th PD and the j-th LED is represented as $d_{i,j}$. Furthermore, $\phi_{i,j}$ is the angle of emission of the j-th LED to the i-th PD with respect to the orthonormal vector of the transmitter plane of the j-th LED. In addition, $\psi_{i,j}$ represents the angle of incidence of the light at the i-th PD from the j-th LED with respect to the orthonormal vector of the receiver plane of the i-th PD. Provided that the LEDs and PDs are placed in a three dimensional Cartesian space, their positions are described by their Cartesian coordinates. The Cartesian coordinates of the j-th LED, $j = 1, \ldots, N_t$, are given from a 3×1 vector which is denoted as $\mathbf{p}^j_t$, while its orientation is given from an orthonormal vector $\mathbf{o}^j_t$ which is vertical to the plane of the LED. In the same way, the Cartesian coordinates of the i-th PD, $i = 1, \ldots, N_r$, are given from a 3×1 vector $\mathbf{p}^i_r$ and its orientation is described from an orthonormal vector $\mathbf{o}^i_r$ which is vertical to the plane of the PD. Therefore, according to [18], $\cos(\phi_{i,j})$ and $\cos(\psi_{i,j})$ can be computed as:

$$\cos(\phi_{i,j}) = \frac{\mathbf{o}^j_t\left(\mathbf{p}^i_r - \mathbf{p}^j_t\right)}{d_{i,j}} \tag{4}$$

and

$$\cos(\psi_{i,j}) = \frac{\mathbf{o}^i_r\left(\mathbf{p}^j_t - \mathbf{p}^i_r\right)}{d_{i,j}}. \tag{5}$$

Finally, the Field of View (FOV) semi-angle of every PD is denoted as $\Psi_{\frac{1}{2}}$.

At the receiver side, DD is utilized as the most practical down-conversion technique. In this case, the optimum Maximum Likelihood (ML) detector of the studied optical MIMO schemes can be expressed as:

$$(\tilde{\mathbf{x}}) = \arg\min_{\mathbf{x}} \|\mathbf{y} - r\mathbf{H}\mathbf{x}\|^2_2. \tag{6}$$

In (6), $\tilde{\mathbf{x}}$ is the detected symbol vector. Provided that $\tilde{\mathbf{x}}$ is detected at the receiver, the transmitted bit-stream can be reconstructed via the deployment of the appropriate demapping process.

A. Optical Space Modulation Techniques

This subsection introduces the operating principles and the main characteristics of the optical space modulation transmission techniques considered in this paper. The optical transmission techniques that are introduced in this subsection are: OSM; OGeSM; and OMS-SM. Note that (1) describes all the previous schemes by using the appropriate design of the transmitted vector $\mathbf{x}$. The following subsections give the design of $\mathbf{x}$ for each considered space modulation technique.

1) Optical Spatial Modulation: Similar to conventional SM in RF communication [13], the main objective of OSM is to promote low complexity system implementation at both communicating ends.

The detailed description of the operating mechanism of OSM is given below. During a symbol period, the transmitted bit-stream is divided into two sequences. The first sequence is composed from $k^{\mathrm{OSM}}_{\mathrm{Space}} = \log_2(N_t)$ bits. At this point, implicitly it is assumed that the number of LEDs is a power of two. In contrast, the length of the second sequence is $k^{\mathrm{OSM}}_{\mathrm{Signal}} = \log_2(M)$, where M is the order of the deployed IM Pulse Amplitude Modulation (PAM) constellation, $\mathcal{M}_{\mathrm{OSM}} = \{s_1, \ldots, s_M\}$. Here, s_k, $k = 1 \ldots, M$, denote the different levels of light intensity transmitted by a LED during the transmission period. Note, that due the operating principle of OSM, none of s_k, $k = 1 \ldots, M$, can have a zero value because

it corresponds to zero intensity light transmission. Otherwise, the zero value would imply the inactivity of a LED, which, as shown below, disregards the OSM transmission principle. In OSM, the first sequence of bits is encoded in the activation of one LED (out of N_r). All the other LEDs remain inactive. Provided that each LED is allocated a unique binary index of length of $k_{\text{Space}}^{\text{OSM}}$, the active LED is the one that possesses the binary index which is equal to the first sequence of bits. The second sequence of bits is encoded in the light intensity transmission of the previously selected LED. Therefore, the spectral efficiency of OSM is $k_{\text{OSM}} = k_{\text{Space}}^{\text{OSM}} + k_{\text{Signal}}^{\text{OSM}}$ bits per channel use (bpcu).

Mathematically, an OSM symbol vector is defined as:

$$\mathbf{x}_{\text{OSM}} = \mathbf{e}_i s_k, \tag{7}$$

where, $\mathbf{e}_i$ is the i-th column of the identity matrix $\mathbf{I}_{N_t,N_t} = [\mathbf{e}_1, \ldots, \mathbf{e}_{N_t}]$. The zero elements of $\mathbf{e}_i$ correspond to the inactive LEDs and the non-zero element corresponds to the active LED. In addition, s_k is the light intensity transmitted from the active LED. At the receiver side, the transmitted OSM symbol vector $\mathbf{x}_{\text{OSM}}$ is detected using (6). In this way, the transmitted bit-stream is reconstructed from the receiver.

Due to its operating principle, OSM requires one transmission chain at the transmitter. In addition, the receiver is able to deploy a low complexity (single stream) ML detector. However, despite the deployment of a single stream detector, OSM has the potential to achieve a multiplexing gain at the expense of additional LEDs.

2) Optical Generalized Spatial Modulation: As described in Section II-A, OSM requires the number of LEDs to be a power of two. However, this constraint is too restrictive. In addition, the activation of a single LED limits the number of encoded bits in only $k_{\text{Space}}^{\text{SM}}$ bits. A solution can be given via the deployment of OGeSM. Note that OGeSM is the incorporation of GeSM in VLC. The GeSM for RF communication is proposed and studied in [15].

In OGeSM, during the signaling period, instead of activating a single LED like OSM, N_a LEDs are active. Here, it holds that $1 < N_a < N_t$. In this way, binary information can be encoded in the combination of the active LEDs. Provided that N_t LEDs are available, from which only N_a are active during a symbol period, a total of $N_c = \binom{N_t}{N_a}$ combinations of active LEDs exists. Note that $\binom{\cdot}{\cdot}$ denotes the binomial coefficient. However, from the N_c combinations, only the $2^{\lfloor \log_2(N_c) \rfloor}$ can be used in order to encode binary information. The selection of the combinations which represent binary information can be done intelligently or randomly. The intelligent selection of the encoded combination can be based on a metric which minimizes the system BER. However, this method results in an additional complexity overhead. This paper, for simplicity, focuses on the random selection of the combinations of active LEDs.

Given that the combinations of active LEDs which encode binary information are selected and each combination is allocated a unique binary index, a total of $k_{\text{Space}}^{\text{OGeSM}} = \log_2\left(2^{\lfloor \log_2(N_c) \rfloor}\right)$ bits are transmitted via the index of the combination of active LEDs. In OGeSM, all of the active LEDs transmit the same light intensity which corresponds to a point drawn from a M-ary IM PAM constellation, $s_k \in \mathcal{M}_{\text{OGeSM}} = \{s_1, \ldots, s_M\}$. Similar to OSM, s_k, $k = 1, \ldots, M$, cannot take a zero value as this corresponds to zero intensity light transmission. Thus, $k_{\text{Signal}}^{\text{OGeSM}} = \log_2(M)$ bits are conveyed to the receiver through the transmission of the standard PAM point s_k. In this way, the spectral efficiency of OGeSM equals to $k_{\text{OGeSM}} = k_{\text{Space}}^{\text{OGeSM}} + k_{\text{Signal}}^{\text{OGeSM}}$ bpcu.

The mathematical formulation of an OGeSM symbol vector is given as:

$$\mathbf{x}_{\text{OGeSM}} = \mathbf{i}_{\text{OGeSM}} s_k, \tag{8}$$

where, $\mathbf{i}_{\text{OGeSM}}$ is a $N_t \times 1$ vector which represents the combination of active LEDs. Note that $\mathbf{i}_{\text{OGeSM}}$ has exactly N_a non-zero elements which are equal to one. All the other elements of $\mathbf{i}_{\text{OGeSM}}$ have a zero value. The position of a non-zero element of $\mathbf{i}_{\text{OGeSM}}$ corresponds to the position of an active LED.

The structure of an OGeSM symbol vector reveals that at the transmitter only one transmission chain is required. Indeed, the same transmission chain can drive all of the active LEDs during the signaling period (because all of the active LEDs transmit the same light intensity). Therefore, the complexity of the transmitter is not affected significantly by the use of OGeSM compared with the use of OSM. However, at the receiver side, the joint inspection of (6) and (8) shows that there is an increase in complexity compared with OSM. This happens because $\mathbf{x}_{\text{OGeSM}}$ is less sparse than $\mathbf{x}_{\text{OSM}}$.

3) Optical Multi-Stream Spatial Modulation: The spectral efficiency of OGeSM can be further increased, if each active LED transmits a different level of light intensity. In this way, a scheme is formed which spatially modulates multiple data streams from the transmitter to the receiver. This scheme is called OMS-SM and is an extension of MS-SM [16] in optical communication. The operating mechanism of OMS-SM determines that during the signaling period a combination of N_a LEDs is activated in order to encode binary information. Therefore, using the same explanation as Section II-A2, it is shown that OMS-SM encodes $k_{\text{Space}}^{\text{OMS-SM}} = \log_2\left(2^{\lfloor \log_2(N_c) \rfloor}\right)$ bits, where $N_c = \binom{N_t}{N_a}$, in the index of the combination of active LEDs. In OMS-SM, each active LED is able to transmit a different level of light intensity. Hence, every active LED is transmitting a different IM PAM symbol, $s_k \in \mathcal{M}_{\text{OMS-SM}} = \{s_1, \ldots, s_M\}$. Here, M stands for the order of the IM PAM constellation $\mathcal{M}_{\text{OMS-SM}}$. In this way, $k_{\text{Signal}}^{\text{OMS-SM}} = N_a \log_2(M)$ bits are conveyed via the N_a PAM points. Thus, the spectral efficiency of MS-SM is $k_{\text{OMS-SM}} = k_{\text{Space}}^{\text{OMS-SM}} + k_{\text{Signal}}^{\text{OMS-SM}}$ bpcu.

The mathematical description of a symbol vector $\mathbf{x}_{\text{OMS-SM}}$ of OMS-SM is given in (9) at the top of the next page. The length of $\mathbf{x}_{\text{OMS-SM}}$ is N_t elements. The i-th element of $\mathbf{x}_{\text{OMS-SM}}$ corresponds to the i-th LED. The operating principle of OMS-SM dictates that $\mathbf{x}_{\text{OMS-SM}}$ has exactly N_a non-zero elements. All the other elements equal to zero. The position of the non-zero elements correspond to the combination of active LEDs during the signaling period. The values of the non-zero elements of $\mathbf{x}_{\text{OMS-SM}}$ represent the light intensity (PAM symbols) transmitted from the corresponding

$$\mathbf{x}_{\text{OMS-SM}} = \Bigg[0,\ldots,0,\ \underbrace{s_1}_{i_1\text{-th position}},0,\ldots,0,\ \underbrace{s_i}_{i_k\text{-th position}},0,\ldots,0,\ \underbrace{s_{N_a}}_{i_{N_a}\text{-th position}}\ 0\ldots,0\Bigg]^T \tag{9}$$

LEDs.

At the receiver side, during a symbol period, the transmitted bit-stream is reconstructed via the detection of the combination of active LEDs and the detection of the N_a PAM points. This is done by deploying the minimization process of (6). Note that the search of (6) is done over all possible symbol vectors of OMS-SM.

The complexity of OMS-SM is higher compared to the complexity of OSM and OGeSM. At the transmitter, N_a communication chains are required in order to produce the different levels of light intensity. Further, at the receiver side, the detection complexity is increased due to the N_a spatially modulated data streams. However, due to the sparsity of (9), it is emphasized that the complexity of an OMS-SM transceiver is lower than the corresponding complexity of a fully spatially multiplexed VLC system. In OSMX, exactly N_t parallel data streams are transmitted during the signaling period.

III. Theoretical Average Bit Error Probability

Section III provides a general theoretical framework which can be used for the evaluation of the ABEP of: OSM; OGeSM; and OMS-SM. This framework is based on the union bound technique [17]. Note that this framework can be easily extended to include the evaluation of the ABEP of any other point-to-point optical MIMO technique.

The union bound technique expresses the ABEP of a point-to-point optical MIMO communication system as:

$$P_{\text{bit}}(\gamma_{\text{e}}) \leq \frac{1}{|\mathcal{B}|k_t}\sum_{\mathbf{x}}\sum_{\substack{\hat{\mathbf{x}}\\ \hat{\mathbf{x}}\neq\mathbf{x}}} d(\mathbf{x}\rightarrow\hat{\mathbf{x}})P_{\text{e}}(\mathbf{x}\rightarrow\hat{\mathbf{x}},\gamma_{\text{e}}). \tag{10}$$

In (10), $P_{\text{bit}}(\gamma_{\text{e}})$ is the ABEP for a given *transmit* electrical SNR. The *transmit* electrical SNR of a VLC system is defined as $\gamma_{\text{e}} = P_o^2/\sigma_{\mathbf{w}}^2$. Without loss of generality and for simplicity, here, it is assumed that the optical transmitted power P_o is normalized to unity (P_o=1). Using this form of normalization, the comparison between the different transmission techniques becomes compact as long as the same normalization is assumed. Obviously, a different normalization results in the same SNR shift for all studied transmission schemes. In addition, $\mathcal{B}$ denotes the transmission alphabet (set of all possible transmitted symbol vectors) of a certain transmission scheme, while $|\mathcal{B}|$ is the size (number of all possible transmitted symbol vectors) of the certain transmission alphabet. Furthermore, k_t denotes the number of bits transmitted per channel use. The Pairwise Error Probability (PEP) of transmitting $\mathbf{x}$ and detecting erroneously $\hat{\mathbf{x}}$, for a given value of γ_{e}, is denoted as $P_{\text{e}}(\mathbf{x}\rightarrow\hat{\mathbf{x}},\gamma_{\text{e}})$. Finally, $d(\mathbf{x}\rightarrow\hat{\mathbf{x}})$ is the number of different bits (Hamming distance) between the bit-word represented by $\mathbf{x}$ and the bit-word represented by $\hat{\mathbf{x}}$.

The inspection of (10) reveals that the assessment of the ABEP requires the evaluation of the PEP between all possible pairs of $\mathbf{x}$ and $\hat{\mathbf{x}}$. In the following, the derivation of the previous PEP is presented. Provided that the detection process is conducted using (6), a symbol error takes place when:

$$\mathcal{E}\left(\mathbf{x},\hat{\mathbf{x}}\right) = \left\{\|\mathbf{y}-r\mathbf{H}\mathbf{x}\|_2^2 > \|\mathbf{y}-r\mathbf{H}\hat{\mathbf{x}}\|_2^2\right\}. \tag{11}$$

After a straightforward elaboration of (11), $\mathcal{E}\left(\mathbf{x},\hat{\mathbf{x}}\right)$ can be re-written as:

$$\mathcal{E}\left(\mathbf{x},\hat{\mathbf{x}}\right) = \left\{-\sum_{i=1}^{N_r}\sum_{j=1}^{N_t}\mathbf{w}_i h_{i,j}\mathbf{c}_i > \frac{r\|\mathbf{H}\mathbf{c}\|_2^2}{2}\right\}, \tag{12}$$

where, $\mathbf{c} = \mathbf{x}-\hat{\mathbf{x}}$ and $\mathbf{c}_i$, $i=1,\ldots,N_t$, is the i-th element of $\mathbf{c}$. Given that $\mathbf{w}_i$, $i=1,\ldots,N_r$, is the i-th element of $\mathbf{w}$ $\left(\mathbf{w}_i \sim \mathcal{N}(0,\sigma_{\mathbf{w}}^2)\right)$, it holds that:

$$-\sum_{i=1}^{N_r}\sum_{j=1}^{N_t}\mathbf{w}_i h_{i,j}\mathbf{c}_i \sim \mathcal{N}\left(0,\sigma_{\mathbf{w}}^2\|\mathbf{H}\mathbf{c}\|_2^2\right). \tag{13}$$

Therefore, using the statistical description of the previous Random Variable (RV), it is shown that the PEP of the pair of $\mathbf{x}$ and $\hat{\mathbf{x}}$ is given as:

$$P_{\text{e}}(\mathbf{x}\rightarrow\hat{\mathbf{x}},\gamma_{\text{e}}) = Q\left(\sqrt{\frac{\|\mathbf{H}\mathbf{c}\|_2^2}{4}r^2\gamma_{\text{e}}}\right), \tag{14}$$

where, $Q\left(\cdot\right)$ is the Q-function. Provided that the Q-function is tightly upper-bounded as [19]:

$$Q\left(x\right) \leq \frac{1}{6}e^{-2x^2} + \frac{1}{12}e^{-x^2} + \frac{1}{4}e^{\frac{-x^2}{2}}, \tag{15}$$

the PEP of (14) can be expressed as in (16), at the top of the next page.

Note that in VLC systems the optical wireless channel is deterministic and does not include any randomness. In fact, multi-path fading is not present due to the size of the detector which is larger than a wavelength [6]. Thus, in contrast to RF communication, there is no need for averaging (16) over the optical channel (which has only one realization for a certain system setup).

In the final remark of Section III, it is emphasized that the ABEP of OSM, OGeSM, and OMS-SM is directly obtained from (10) via the use of (16). This is done by setting the appropriate values for $|\mathcal{B}|$ and k_t. For each considered transmission scheme, the values for the previous quantities are given in detail in Sections II-A1 to II-A3.

IV. Results and Discussion

This section provides Monte Carlo simulation results that assess the performance of: OSM; OGeSM; and OMS-SM. In addition, the simulation results are verified using the bounds of the theoretical analysis of Section III.

$$P_{\mathrm{e}}(\mathbf{x} \to \hat{\mathbf{x}}, \gamma_{\mathrm{e}}) \leq \frac{1}{6} e^{-\frac{\|\mathbf{Hc}\|_2^2}{2} r^2 \gamma_{\mathrm{e}}} + \frac{1}{12} e^{-\frac{\|\mathbf{Hc}\|_2^2}{4} r^2 \gamma_{\mathrm{e}}} + \frac{1}{4} e^{-\frac{\|\mathbf{Hc}\|_2^2}{8} r^2 \gamma_{\mathrm{e}}}. \quad (16)$$

TABLE I
COORDINATES OF LEDS AND PDS.

Transmitter Coordinates (in m)				Receiver Coordinates (in m)			
	x-axis	y-axis	z-axis		x-axis	y-axis	z-axis
LED 1	2.2	1.8	3.5	PD 1	2.15	1.85	0.85
LED 2	1.8	1.8	3.5	PD 2	1.85	1.85	0.85
LED 3	1.8	2.2	3.5	PD 3	1.85	2.15	0.85
LED 4	2.2	2.2	3.5	PD 4	2.15	2.15	0.85

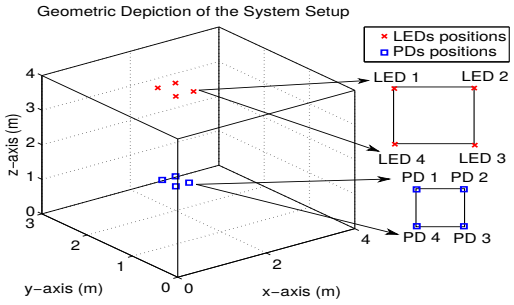

Fig. 1. Visual representation of the considered 4×4 VLC system.

For the purpose of comparison, two benchmark systems are considered. The first benchmark system is OSMX. In an OSMX system, the transmitter conveys N_t parallel data streams to the receiver. Therefore, every symbol period, binary information is transmitted via N_t points drawn from a M-ary IM PAM constellation. The second benchmark system is ORC. The operating principle of ORC determines that all of the transmitting LEDs emit the same light intensity. In this way, a single point of a M-ary IM PAM constellation conveys binary information from the transmitter to the receiver. Note that there is a difference between the deployed IM PAM constellation of a space modulation technique and the corresponding PAM constellation of the benchmark systems. In the benchmark systems, a M-ary IM PAM constellation is constituted from the following set of points, $\mathcal{M}_{\mathrm{bs}} = \{s_0, \ldots, s_{M-1}\}$, where $s_0 = 0$ (zero light intensity). In contrast, as stated in Section II, the points of a PAM constellation deployed by a space modulation take only non-zero values. However, in order to enforce a fair comparison between all transmission schemes, the transmitted symbol vector $\mathbf{x}$ is normalized to the same average optical power. Finally, the detector of the benchmark systems is based on the ML principle. Thus, their detector is given from (6).

An indoor three dimensional space is considered where four transmitting LEDs and four receiving PDs are placed. The coordinates of the LEDs and PDs are given in Table I. The visual representation of the considered 4×4 ($N_t = 4$ and $N_r = 4$) VLC system is given in Fig. 1. The orientation of all the LEDs is given from the following orthonormal vector, $\mathbf{o}_t = [0, 0, -1]^T$, while the orientation of all the PDs is given as, $\mathbf{o}_r = [0, 0, 1]^T$. Furthermore, the transmitter semi-angle, $\Phi_{\frac{1}{2}}$, is 15 degrees. The area of each PD is 1 cm^2. The value of the responsivity of the PDs is $r = 0.4$ A/W. Finally, the FOV of the PDs, $\Psi_{\frac{1}{2}}$, is 30 degrees.

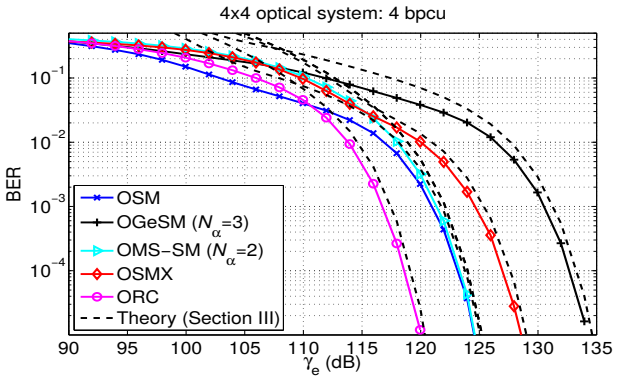

(a) BER versus γ_e (dB) of a 4×4 system with spectral efficiency 4 bpcu.

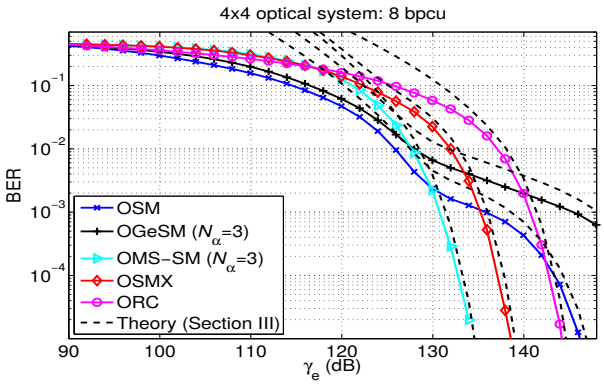

(b) BER versus γ_e (dB) of a 4×4 system with spectral efficiency 8 bpcu.

Fig. 2. Performance evaluation of the considered space modulation techniques (OSM, OGeSM, and OMS-SM) against the benchmark systems (OSMX and ORC). The system setup is 4×4 with spectral efficiency 4 and 8 bpcu. The solid lines correspond to simulation results, while the dashed lines correspond to the upper bounds derived in Section III.

Fig. 2(a) and 2(b) present the performance of the studied VLC system when the spectral efficiency is 4 bpcu and 8 bpcu, respectively. In each case, the spectral efficiency is set to the desired value by selecting the appropriate order of the employed IM PAM constellation. The metric of BER is plotted versus the *transmit* electrical SNR (as defined in Section III). Note that, due to the effect of the pathloss of the optical channel, the *detection* SNR at the side of the receiver faces a significant reduction with respect to the *transmit* electrical SNR. For this reason, the *transmit* electrical SNR (γ_e) in Fig. 2(a) and 2(b) takes high values.

As shown in Fig. 2(a) and 2(b), the analytical bounds of Section III are tight in relative high electrical SNR. In relative low electrical SNR, the theoretical bounds demonstrate a gap from the simulated curves. However, this phenomenon is a well known characteristic of the union bound technique deployed

in Section III [17]. Note that the theoretical ABEP of the benchmark systems is also evaluated following the framework of Section III. The is done by setting the appropriate values for $\mathcal{B}$ and k_t.

The inspection of Fig. 2(a) shows that the best BER performance in relative low SNRs ($\gamma_e < 110.5$ dB) is achieved by OSM. In contrast, as the value of SNR is increased above 110.5 dB, ORC has the best BER performance. The reason that ORC outperforms the other schemes is its operating principle, which resembles Single-Input Single-Output (SISO) communication. In SISO communication, only one symbol is conveyed from the transmitter to the receiver, just like ORC. In general, MIMO communication undergoes a performance degradation when the similarity between the existing sub-channels is high. Indeed, the channel similarity in the studied system setup is high due to the small spacing of the LEDs and PDs, and their symmetrical deployment. In fact, this is also the reason that OSM and OMS-SM outperform OSMX. The results in Fig. 2(a) show that OSM and OMS-SM are more robust compared to OSMX to channel similarity. Furthermore, Fig. 2(a) demonstrates that OSM outperforms OMS-SM for the same reason. In fact, OMS-SM is more prone to performance degradation due to channel similarity. This happens because OMS-SM spatially modulates multiple data streams. In relative high SNR, the worst performance is achieved by OGeSM.

Fig. 2(b) demonstrates that, even when the spectral efficiency is increased to 8 bpcu, OSM outperforms all the other schemes in relative low SNR ($\gamma_e < 129.8$ dB). However, at 129.8 dB, there is a crossing point after which OMS-SM becomes the most efficient transmission scheme. In fact, as shown in Fig. 2(b), for a BER=10^{-4}, OMS-SM exhibits an electrical SNR gain of about 5 dB compared to the OSMX. Fig. 2(b) shows that OSMX is the second most efficient scheme in relative high SNR. Furthermore, in relative high SNR, the performance of OSM, OGeSM, and ORC becomes worse compared to OSMX and OMS-SM. This is due to the higher order of the deployed constellation of OSM, OGeSM, and ORC. More specifically, OMS-SM, OSMX, OSM, OGeSM, and ORC use a constellation order of 4, 4, 64, 64, and 256, respectively. Therefore, it can be concluded that, in relative high SNR and for high spectral efficiency, it is preferable to exploit the multiplexing gain of OMS-SM and OSMX instead of the robustness of ORC and OSM to channel similarity. Finally, Fig. 2(b) shows that OGeSM gives the worst BER performance in values of SNR above 140 dB.

V. Conclusions

In this paper, the BER performance of OSM, OGeSM, and OMS-SM is studied against the corresponding performance of the benchmark systems of ORC and OSMX. The performance evaluation was conducted using both simulation and analytical results. As regard the theoretical results, tight upper bounds for the ABEP of all considered optical MIMO transmission schemes are provided. In this way, the provided simulation result are confirmed. For the studied system setup, it was concluded that OSM exhibits the best BER performance among the different schemes in relative low SNR. It was inferred that as SNR increases and the spectral efficiency is also increased, the performance of OMS-SM becomes the best one.

Acknowledgement

Prof. Harald Haas acknowledges support by EPSRC under grant EP/K008757/1.

References

[1] D. Tsonev, S. Videv, and H. Haas, "Light Fidelity (Li-Fi): Towards All-Optical Networking," in *Proc. SPIE, Broadband Access Commun. Technol. VIII*, vol. 9007, Dec. 18 2013. [Online]. Available: http://dx.doi.org/10.1117/12.2044649

[2] H. Chun, P. Manousiadis, S. Rajbhandari, D. Vithanage, G. Faulkner, D. Tsonev, J. McKendry, S. Videv, E. Xie, E. Gu, M. Dawson, H. Haas, G. Turnbull, I. Samuel, and D. O'Brien, "Visible Light Communication Using a Blue GaN LED and Fluorescent Polymer Color Converter," *IEEE Photon. Technol. Lett.*, vol. 26, no. 20, pp. 2035–2038, Oct. 2014.

[3] D. Tsonev, H. Chun, S. Rajbhandari, J. McKendry, S. Videv, E. Gu, M. Haji, S. Watson, A. Kelly, G. Faulkner, M. Dawson, H. Haas, and D. O'Brien, "A 3-Gb/s Single-LED OFDM-Based Wireless VLC Link Using a Gallium Nitride μLED," *IEEE Photon. Technol. Lett.*, vol. 26, no. 7, pp. 637–640, Apr. 2014.

[4] L. Zeng, D. O'Brien, H. Minh, G. Faulkner, K. Lee, D. Jung, Y. Oh, and E. T. Won, "High Data Rate Multiple Input Multiple Output (MIMO) Optical Wireless Communications Using White LED Lighting," *IEEE J. Sel. Areas Commun.*, vol. 27, no. 9, pp. 1654–1662, Dec. 2009.

[5] G. J. Foschini and M. J. Gans, "On Limits of Wireless Communications in a Fading Environment when Using Multiple Antennas," *Wireless Personal Communications*, vol. 6, no. 6, pp. 311–335, 1998.

[6] J. M. Kahn and J. R. Barry, "Wireless Infrared Communications," *Proc. IEEE*, vol. 85, no. 2, pp. 265–298, Feb. 1997.

[7] T. Fath and H. Haas, "Performance Comparison of MIMO Techniques for Optical Wireless Communications in Indoor Environments," *IEEE Trans. on Commun.*, vol. 61, no. 2, pp. 733–742, February 2013.

[8] ——, "Optical Spatial Modulation Using Colour LEDs," in *Proc. of the IEEE 2013 Intern. Conf. on Commun. (ICC)*, June 2013, pp. 3938–3942.

[9] R. Mesleh, R. Mehmood, H. Elgala, and H. Haas, "Indoor MIMO Optical Wireless Communication Using Spatial Modulation," in *IEEE International Conference on Communications (ICC)*, Cape Town, South Africa, May 22–27 2010, pp. 1–5.

[10] Z. Yu, R. Baxley, and G. Zhou, "Multi-User MISO Broadcasting for Indoor Visible Light Communication," in *Proc. of the 2013 IEEE Intern. Conf. on Acoust., Speech and Signal Proc. (ICASSP)*, May 2013, pp. 4849–4853.

[11] K.-H. Park, Y.-C. Ko, and M. Alouini, "On the Power and Offset Allocation for Rate Adaptation of Spatial Multiplexing in Optical Wireless MIMO Channels," *IEEE Trans. on Commun.*, vol. 61, no. 4, pp. 1535–1543, April 2013.

[12] H. Ma, L. Lampe, and S. Hranilovic, "Robust MMSE Linear Precoding for Visible Light Communication Broadcasting Systems," in *Proc. of the 2013 IEEE Globecom Workshops*, Dec 2013, pp. 1081–1086.

[13] M. Di Renzo, H. Haas, A. Ghrayeb, S. Sugiura, and L. Hanzo, "Spatial Modulation for Generalized MIMO: Challenges, Opportunities, and Implementation," *Proc. IEEE*, vol. 102, no. 1, pp. 56–103, Jan 2014.

[14] A. Stavridis, S. Sinanović, M. D. Renzo., and H. Haas, "Energy Evaluation of Spatial Modulation at a Multi-Antenna Base Station," in *Proc. of the 78th IEEE Veh. Tech. Conf. (VTC)*, Las Vegas, USA, Sep. 2–5, 2013.

[15] A. Younis, N. Serafimovski, R. Mesleh, and H. Haas, "Generalised Spatial Modulation," in *Asilomar Conf. on Signals, Systems, and Computers*, Pacific Grove, CA, USA, Nov. 2010.

[16] J. Wang, S. Jia, and J. Song, "Generalised Spatial Modulation System with Multiple Active Transmit Antennas and Low Complexity Detection Scheme," *IEEE Trans. on Wireless Commun.*, vol. 11, no. 4, pp. 1605 – 1615, April 2012.

[17] J. G. Proakis and M. Salehi, *Communication System Engineering*. Prentice Hall, 1994.

[18] J. Barry, J. Kahn, W. Krause, E. Lee, and D. Messerschmitt, "Simulation of Multipath Impulse Response for Indoor Wireless Optical Channels," *IEEE J. Select. Areas Commun.*, vol. 11, no. 3, pp. 367–379, Apr. 1993.

[19] M. Chiani, D. Dardari, and M. K. Simon, "New Exponential Bounds and Approximations for the Computation of Error Probability in Fading Channels," *IEEE Trans. on Wireless Commun.*, vol. 2, no. 4, pp. 840–845, July 2003.